



<http://dx.doi.org/10.35596/1729-7648-2023-21-2-77-85>

Original paper

UDC 621.384.3

DESIGN AND PERFORMANCE OF AMORPHOUS SILICON BASED ON UNCOOLED BOLOMETER-TYPE INFRARED FOCAL PLANE ARRAYS

TRAN VAN TRIEU¹, VIKTOR R. STEMPIITSKY¹, IVAN YU. LOVSHENKO¹,
KIRILL V. KORSAK¹, DAO DINH HA²

¹Belarusian State University of Informatics and Radioelectronics (Minsk, Republic of Belarus)

²Le Quy Don University of Science and Technology (Hanoi, Vietnam)

Submitted 30.01.2023

© Belarusian State University of Informatics and Radioelectronics, 2023

Белорусский государственный университет информатики и радиоэлектроники, 2023

Abstract: Uncooled bolometric type thermal detectors, combined into a matrix and placed into a focal plane array have the following characteristics: low cost, operation at room temperature, compatibility with the silicon CMOS technology, and high detecting performance; therefore recently it became a hot spot in infrared or terahertz detection field. The performance of uncooled infrared focal plane detector arrays depends on the optimization of critical parameters which are determined by geometrical design and the electrical, optical, and thermal physical properties of the detector materials. We report the study of a fabrication process and characterization of two (2D) dimensional arrays of uncooled microbolometers based on silicon (α -Si) thermo-sensing films. Because these arrays substantially reduce sensor size, they are becoming the preferred format for most modern applications.

Keywords: detector, uncooled microbolometer, infrared detector, thermo-sensing, amorphous silicon, modeling.

Conflict of interests. The authors declare no conflict of interests.

Gratitude. The research was carried out with financial support and as part of solving the tasks of assignment 3.3 of the State research program “Photonics and electronics for innovation” along with JSC “INTEGRAL” – manager holding company “INTEGRAL”. The authors express their gratitude to Vladimir Kolos for his help in preparing this paper.

For citation. Tran Van Trieu, Stempitsky V. R., Lovshenko I. Yu., Korsak K. V., Dao Dinh Ha (2023) Design and Performance of Amorphous Silicon Based on Uncooled Bolometer-Type Infrared Focal Plane Arrays. *Doklady BGUIR*. 21 (2), 77–85. <http://dx.doi.org/10.35596/1729-7648-2023-21-2-77-85>.

КОНСТРУКЦИЯ И ХАРАКТЕРИСТИКИ НЕОХЛАЖДАЕМЫХ БОЛОМЕТРИЧЕСКИХ ИНФРАКРАСНЫХ РЕШЕТОК НА ОСНОВЕ АМОРФНОГО КРЕМНИЯ

ЧАН ВАН ЧИЕУ¹, В. Р. СТЕМПИЦКИЙ¹, И. Ю. ЛОВШЕНКО¹,
К. В. КОРСАК¹, ДАО ДИНЬ ХА²

¹Белорусский государственный университет информатики и радиоэлектроники
(г. Минск, Республика Беларусь)

²Вьетнамский государственный технический университет имени Ле Куи Дона (Ханой, Вьетнам)

Поступила в редакцию 30.01.2023

Аннотация. Неохлаждаемые тепловые детекторы болометрического типа, объединенные в матрицу, размещенную в фокальной плоскости, в последнее время активно применяются в инфракрасном или терагерцовом поле обнаружения, поскольку обладают низкой стоимостью и высокой эффективностью обнаружения, совместимы с кремниевой КМОП-технологией, а также работают при комнатной температуре. Характеристики таких детекторов зависят от оптимизации критических параметров, которые определяются геометрической конструкцией, электрическими, оптическими и тепловыми свойствами применяе-

мых материалов. В статье рассмотрены эксплуатационные характеристики пикселей двумерных массивов неохлаждаемых микроболометров на основе термочувствительных пленок аморфного кремния. Поскольку эти массивы значительно уменьшают размер сенсора, они становятся предпочтительным форматом для большинства современных приложений.

Ключевые слова: детектор, неохлаждаемый микроболометр, инфракрасный детектор, термодатчик, аморфный кремний, моделирование.

Конфликт интересов. Авторы заявляют об отсутствии конфликта интересов.

Благодарность. Исследования выполнены при финансовой поддержке и в рамках решения задач задания 3.3 Государственной программы научных исследований «Фотоника и электроника для инноваций» совместно с ОАО «ИНТЕГРАЛ» – управляющая компания холдинга «ИНТЕГРАЛ». Авторы выражают благодарность Владимиру Колосу за помощь в подготовке статьи.

Для цитирования. Конструкция и характеристики неохлаждаемых болометрических инфракрасных решеток на основе аморфного кремния / Чан Ван Чиеу [и др.] // Доклады БГУИР. 2023. Т. 21, № 2. С. 77–85. <http://dx.doi.org/10.35596/1729-7648-2023-21-2-77-85>.

Introduction

Infrared (IR) detectors can be divided into two groups: the photon type and the thermal type. Uncooled thermal detectors have several advantages over photon detectors in that an uncooled IR camera is compact, light-weight, inexpensive, and reliable, and it hardly needs any maintenance. Their main shortcomings are lower sensitivity and longer response time. However, both of these problems have almost been solved, with the advent of surface micromachining technology as well as reliable deposition techniques for thin films. Micromachining technology offers the fabrication of good thermal isolation structures, e. g., a micro bridge structure. IR technology has been widely investigated but still it is an important field of study, while trying to satisfy the need of low cost and high-performance IR imaging systems. Microbolometer based on micro bridge structure has characteristics of low power, low cost, working at room temperature, high reliability and high detecting performance which is widely used in military and civilian fields [1–3].

There are mainly two kinds of microbolometers currently depending on whether the thermal sensitive material is vanadium oxide (VO_x) or α -Si [4]. VO_x , polycrystalline silicon, germanium and hydrogenated α -Si are materials commonly employed for microbolometer sensors [5–7]. Among available sensor materials, α -Si has been widely utilized for its good temperature coefficient of resistance (TCR), mechanical strength, low thermal mass, and high manufacturing yield, as well as full compatibility with the CMOS processes. Those features enable shrinking pixel size which results in several technological advances as: larger format arrays, smaller and cheaper optical systems and packages [8]. In this article, the Coventor software was used to calculate design and fabrication bolometer based on micro-bridge for IR detecting. For IR detecting, micro bridge structure based on $16 \times 16 \mu\text{m}^2$ α -Si thermo-sensing films was designed and fabricated.

Approach, design, and fabrication

Technical evolution of the microbolometer is occurring in various fields such as pixel design, IR optics, and packaging [9]. Main motivations driving this evolution are to reduce cost and to increase integration. Normal structure of the microbolometer consists of one suspended multi-layer membrane and long supporting legs. The membrane, including dielectric material layer, thermal sensitive material layer, electrode layer and absorption layer, can absorb incident infrared radiation and cause multi-layer film membrane temperature change of the micro-bridge. A microbolometer requires an active material with high TCR, which means that small changes in the temperature of the thermo-sensing material translate into large changes in resistance. Low electrical resistivity is required in order to obtain minimized Johnson noise and good compatibility of the detector with the read-out circuitry, thus increasing the signal-to-noise ratio [10]. In general, an infrared detector generates temperature changes by absorbing infrared light from the external environment and converts those changes into an electrical signal, so the infrared absorption structure plays an important role in enhancing detector sensitivity. Minimization of mechanical deformation in unit pixels is important to maintain the optically resonant cavity structure and electrical uniformity through the membrane. There are three mechanisms of heat transfer that occur in a thermal detector, such as:

- 1) conduction mechanisms, which occur when the heat flows from the thermo-sensing area along the supporting legs to the substrate;
- 2) convection which occurs when the heat flows in the presence of a surrounding atmosphere; this mechanism is not very important if the detector is encapsulated in a vacuum package;
- 3) radiation mechanism is presented by the fact that the detector radiates energy back to its surroundings and the surroundings radiate back to it.

When the microbolometers are encapsulated in an evacuated package, with an IR transmitting window, convection and radiation mechanism are minimized. Thus, the main heat loss mechanism is the conduction from the thermo-sensing material to the substrate through the supporting structure. The supporting structure is a very important part of thermal detectors, it provides three functions: mechanical support, electrical conducting path and thermal conducting path. The development of arrays of uncooled IR sensors depends on the ability to form thermal isolation structures which should be compact, robust, and easy to fabricate. MEMS technology greatly contributed to the reduction of thermal conductance and sensitivity improvement. The value of output electric signal is related to the tiny temperature change of membrane. According to the detector operating at vacuum and room temperature conditions, thermal convection and thermal radiation could be ignored in the calculation process, so the thermal conductance (G) of microbolometer is the total thermal conduction between a bolometer and its surrounding and it can be estimated by

$$G = G_{leg-conduction} + G_{radiation} + G_{gas-conduction} + G_{convection}, \quad (1)$$

where $G_{leg-conduction}$, $G_{radiation}$ is the thermal conduction between the bolometer and its surrounding through the bolometer legs and by emitted heat radiation; $G_{gas-conduction}$, $G_{convection}$ is the thermal conduction between the bolometer and its surrounding through the gas and by gas convection.

According to the detector operating at vacuum and room temperature condition, thermal convection and thermal radiation could be ignored in the calculation process, so the thermal conductance G of microbolometer is

$$G \approx 2G_{leg} = 2k \frac{wd}{l}, \quad (2)$$

where G_{leg} is the thermal conductance of micro-bridge leg; k is thermal conductivity of the supporting leg; w , d , l are the width, thickness, and length of the leg, respectively.

Thermal capacity C of the membrane can be expressed as

$$C = \sum V_i \rho_i c_i, \quad (3)$$

where V_i , ρ_i , c_i are the volume, density and specific heat capacity of the multi-layer thin film in the membrane.

The response time τ of micro-bridge can be calculated with thermal conductance and thermal capacity

$$\tau = \frac{C}{G}. \quad (4)$$

The response time is related to the working frequency. And then the other parameters can be calculated according to the requirement of the response time. The relative TCR is defined as

$$\alpha = \frac{1}{R} \frac{dR}{dT}. \quad (5)$$

The change of voltage of a constant current-biased bolometer is

$$\Delta V = I \Delta R = IR \alpha \Delta T. \quad (6)$$

Performance of microbolometers is evaluated through voltage responsivity R_v , noise, and directivity. Voltage responsivity is the output signal generated per unit of incident power, expressed by

$$R_v = \frac{\eta \beta I \alpha R_{ef}}{G_{th} \sqrt{1 + \omega^2 \tau_{th}^2}}, \quad (7)$$

where η is absorption coefficient; β is the fill factor; I is the bias current; α is the TCR of the thermo-sensing film; R_{ef} stands for an effective resistance resulting from the equivalent parallel resistance between

bolometer and readout circuit impedance; G_{th} is the thermal conductance; ω is the angular frequency of the signal modulation; τ_{th} is the thermal time constant (also called response time).

R_v can also be determined by the formula

$$R_v = \frac{\Delta V}{P_{in}}, \quad (8)$$

where ΔV is the voltage difference from dark to infrared; P_{in} is the infrared power.

To provide a high absorption of the radiation in the bolometer membrane, conventional bolometers contain resonant optical cavity (Fabry-Perot) structures that are optimized for the targeted wavelength. The most commonly used resonant optical cavity design, in which the infrared mirror (typically aluminum) of the resonant optical cavity is placed on the surface of the underlying substrate (the ROIC) and the bolometer membrane is placed at the distance d of $\lambda/4$ from the mirror surface on the substrate. Thus, a high fraction of the incident infrared radiation at a specific wavelength λ is absorbed in the bolometer membrane [11]. For a targeted wavelength interval of 8 to 14 μm , the distance between the bolometer membrane and the mirror on the substrate is typically about 2 to 2.5 μm [11, 12]. During a system-level simulation, all of the above parameters should be considered.

Examples of fabricated detectors and arrays

The pixel is divided into two parts (Fig. 1), a silicon (Si) readout integrated circuit in the lower part and a suspended micro bridge structure in the upper part.

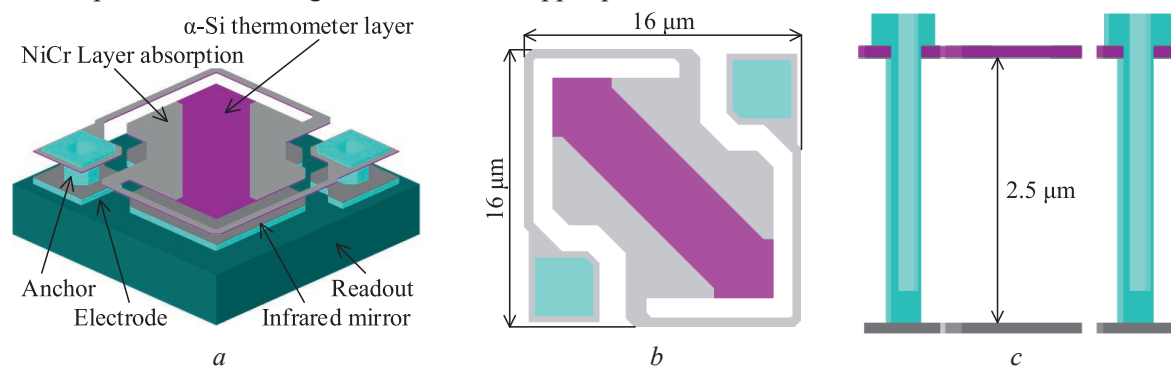


Fig. 1. Structure of the microbolometer pixel: *a* – 3D model; *b* – top view; *c* – cross-section

The bolometer is composed of a thermometer integrated on a micro-bridge. This micro-bridge is supported by two legs anchored over the silicon substrate by metal studs. This micro-bridge is built on a sacrificial layer which is removed in a final step. The distance between the ROIC and the micro-bridge is 2.5 μm . This vacuum gap works as a quarter wavelength cavity, which sets the detector spectral response maximum at a wavelength close to 10 μm . The active region of the sensor consists of the IR absorber layer, made of NiCr, which absorbs incident radiation, and an underlying thermometer layer, comprised of α -Si, whose sheet resistance will vary as a function of the temperature change induced by the absorption of radiation by the NiCr layer. Considered structure has a pixel step is 16 μm , NiCr supporting legs width is 1 μm , α -Si and NiCr film thickness is 0.1 μm and 15 nm accordingly. Active area of pixel is 197 μm^2 . The Tab. 1 shows the parameters of the materials used in modeling.

Table 1. Material properties of microbolometer

Material	Elastic constants (Elastic-Iso)		Density, $\text{kg}/\mu\text{m}^3$	Stress (MPa) – AnIso			Thermal conduction G , $\text{pW}/(\mu\text{m}\cdot\text{K})$	Specific heat C , $\text{pJ}/(\text{kg}\cdot\text{K})$	Electric conduction, $\text{pS}/\mu\text{m}$
	E , MPa	Poisson		S_x	S_y	S_z			
Al	$7.7 \cdot 10^4$	0.3	$2.3 \cdot 10^{-15}$	24	14	0	$2.37 \cdot 10^8$	$8.98 \cdot 10^{14}$	$3.69 \cdot 10^{13}$
NiCr	$1.0 \cdot 10^4$	0.2	$4.6 \cdot 10^{-15}$	-160	-160	0	$2.08 \cdot 10^7$	$5.0 \cdot 10^{14}$	$2.83 \cdot 10^{12}$
α -Si	$8.0 \cdot 10^4$	0.3	$2.26 \cdot 10^{-15}$	17	17	0	$1.0 \cdot 10^6$	$6.81 \cdot 10^{14}$	Variable value

Besides its silicon technology compatibility, α -Si presents many other advantages. First, it enables the manufacturing of very thin suspended membranes combined with short leg lengths resulting in high fill factor and high mechanical strength structures that could sustain high vibration rates and high mechanical shocks. This reduced mechanical susceptibility to vibration or shock solicitation is obviously

important for a number of military as well as commercial applications. Secondly, the very thin thermally isolated suspended membrane, along with the low thermal mass of silicon, results in a very low pixel thermal time constant. Finally, this simple technology leads to high manufacturing yield and therefore low manufacturing cost.

Results and discussions

Minimizing heat loss mechanisms is essential to maximizing sensitivity. The dominant heat loss mechanism is heat conduction through the support structure to the underlying substrate. The total thermal conductance G can be determined by means of a steady-state thermal analysis in which a constant power input is supplied via a heat flux surface boundary condition. G is the ratio of the total power supplied and the maximum temperature change achieved by the sensor. Fig. 2 shows the calculation model of thermal conductance.

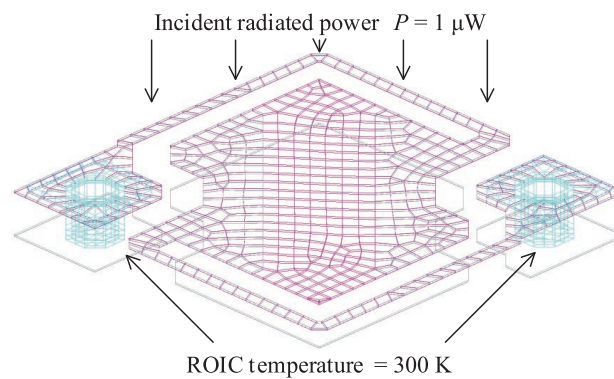


Fig. 2. The calculation model of thermal conductance

Results calculated by Coventor software

$$G = \frac{\text{Input Power}}{\Delta T} = 9.84 \cdot 10^{-8} \text{ W/K.}$$

The time constant, τ , provides measurement of the response time of the sensor; τ needs to be sufficiently low to satisfy the application requirements of the microbolometer. The time constant can be determined from a transient thermal analysis by examining the temperature response of the sensor as a function of time upon cooling down from the maximum steady-state temperature computed from the previous analysis. The time constant can be determined from a transient thermal analysis by examining the temperature response of the sensor as a function of time upon cooling down from initial ROIC temperature of 310 to 300 K (Fig. 3). The time constant $\tau = 380 \mu\text{s}$. With both G and τ known, C the total heat capacity can be calculated using equation (3):

$$C = G\tau = 9.84 \cdot 10^{-8} \cdot 0.38 \cdot 10^{-3} = 3.74 \cdot 10^{-11} \text{ J/K.}$$

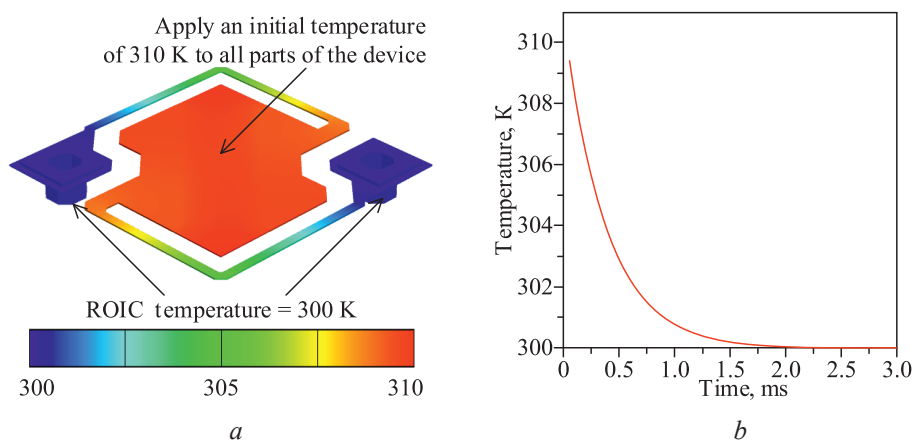


Fig. 3. The calculation model of time constant (a) and the time constant of microbolometer (b)

During operation, a bias voltage signal is applied across the sensor, inducing a current through the thermometer layer, which depends on the temperature-dependent resistance that changes as incident radiation is absorbed. Thus, in addition to the fundamental thermal design parameters previously discussed, comprehending the response of the sensor to an applied voltage is essential. The static voltage-temperature ($V-T$) curve allows designers to understand the effect of Joule heating on the microbolometer and to determine the temperature gain of the microbolometer at steady state when a given potential is applied across it. Understanding the steady-state current-voltage ($I-V$) curve, whose slope is the resistance of the microbolometer, is important as the resistance contributes to the sensitivity of the device. A single, steady-state electrothermal analysis is used to generate both the $I-V$ and $V-T$ curves by sweeping the applied voltage from -2 to 2 V in steps of 0.1 V, applied across the microbolometer anchor surfaces (Fig. 4). Fig. 4, *a* illustrates how the static temperature of the device will vary due to a constant voltage drop across the resistive sensor and the current that is induced in the resistive sensor at each applied voltage plot the resistance as a function of temperature.

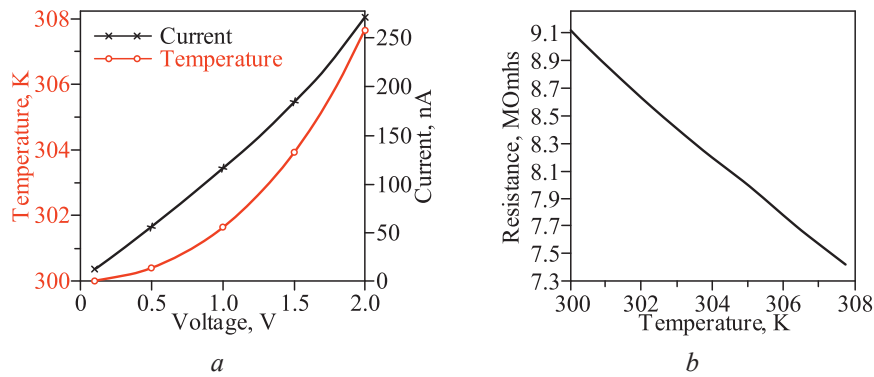


Fig. 4. Illustrates curvature properties

From Fig. 4, *b* it allows to calculate the α , used in equation (5). As shown above, resistance changes quite linearly with temperature. The linear relationship between resistance and temperature allows us to use the value of the $\alpha \approx -0.028$.

In addition to the thermal and electrical properties examined so far, understanding the mechanical stiffness of the sensor is essential. Microbolometers are designed to stand exactly a quarter wavelength of the incident IR radiation from the substrate. This design specification is required because some radiation passes through the sensor, reflects from the substrate, and impinges on the back of the sensor. A gap of a quarter wavelength maximizes the superposition of the reflected wave with the initial wave, thus maximizing absorption by the sensor. Deformation can cause the sensor to deviate from this specification. Deformation results when the mechanical stiffness of the device is balanced against the resolution of residual stresses from fabrication, as well as elevated temperatures causing the sandwiched layers comprising the sensor to expand and contract differently, which is caused by varying coefficients of thermal expansion. The flatness of the sensor can be assessed by a steady-state mechanical analysis. Using the grid model (Fig. 5) there is the run a coupled thermomechanical analysis. A coupled thermomechanical analysis will capture the effects of thermal expansion/contraction in addition to the deformation due the pre-stresses.

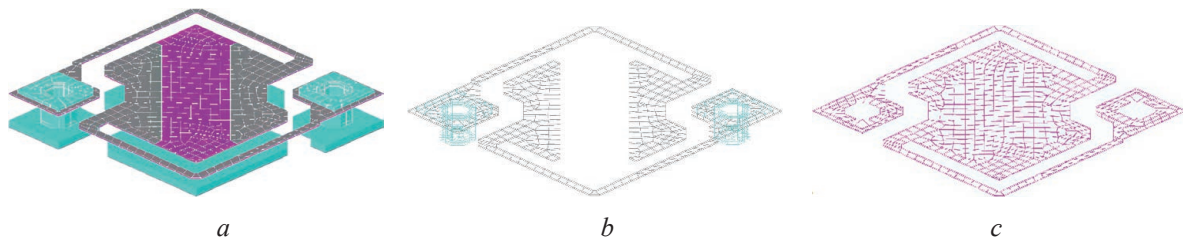


Fig. 5. The mesh model of microbolometer: *a* – 3D mesh model; *b* – electrode Al and NiCr layer; *c* – α -Si resistance layer

The results show that the highest and lowest elevations of the IR absorbing layer differ by nearly 3 nm across the pixel. This result ensures the maintenance of the superposition of the reflected wave with the initial wave. Applying equation (7) with assumed values required to determine responsivity

includes: bias current $I = 10^{-6}$ A is arbitrarily chosen as a representative bias current; ω – the angular frequency of modulation of the radiation, is assumed to be 60 Hz; η – the absorbance of the IR sensitive layer, is the product of the absorption of the NiCr, α -Si layer and the fill factor of the sensor, taken as 0.9 and 0.77, respectively. So, value of sensitivity is equal to $R_v = 2.33 \cdot 10^6$ V/W. In summary, the microbolometer parameters are presented in Tab. 2.

Table 2. Results of survey of the parameters of the above designed bolometer

Design parameter	Value
Thermal conductance G , W/K	$9.84 \cdot 10^{-8}$
Thermal time constant τ , s	$0.38 \cdot 10^{-3}$
Specific heat C , J/K	$3.74 \cdot 10^{-11}$
Resistance R (for 300 K), Omhs	$9.11 \cdot 10^6$
Thermal coefficient of resistance (TCR), 1/K	-0.028
Maximum deflection (for 300 K), μm	0.003
Fill factor of the sensor β	0.77
Responsivity R_v , V/W	$2.33 \cdot 10^6$

Simulating the operation of a microbolometer requires analyzing multiple coupled physical domains. Incident radiation absorption causes a temperature increase, which mechanically deforms the device, but also changes the resistance of the thermometer layer. The change in the resistance is detected by means of the output current through or voltage drop across the microbolometer, which is incorporated into an integrated circuit. Thus, coupling between mechanical, electrical, and thermal domains is required. Next, we need to conduct a steady-state electro-thermomechanical simulation. To do this, a power supply with a voltage of 1 μV is connected to the one of the electrodes of the bolometer, and the power of the incident voltage varies from 0 to 1 $\text{pW}/\mu\text{m}^2$. Fig. 6 shows the change in mechanical deformation, resistance, and current through the microbolometer as the input radiated power increases.

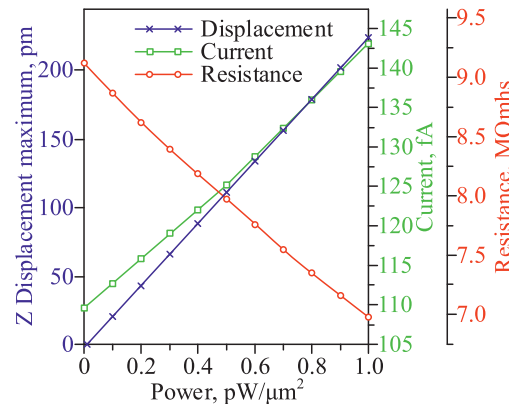


Fig. 6. The mechanical deformation, resistance, and current of the microbolometer as the input incident radiated power increases

Microbolometers operate under a voltage bias, thus allowing for the detection of output current, which is a function of the sensor resistance. However, the application of this voltage signal induces Joule heating, which should be understood independently of the temperature increase due to the absorbed IR radiation. Given that the voltage signal will be time-dependent, we will run a transient electrothermal simulation to predict the thermal response of the microbolometer to an input voltage pulse. The voltage profile that will be applied to the device is shown in Fig. 7, a. The voltage pulse applies a bias of 1 V, transition time 40 μs , the duration designed to allow the sensor temperature to ramp up to the steady-state value predicted in accordance with the thermal time constant inherent to the device.

The plot fig. 7, b shows that the device reaches a maximum temperature of 302.98 K due to the Joule heating induced by the voltage pulse. After the voltage signal is removed, the device temperature drops back to 300 K as the heat is lost to the substrate by conduction through the anchor surfaces. In practice, an electrical circuit is used to detect incident radiation that is absorbed by the microbolometer. When the microbolometer is exposed to incident radiation, the temperature increases and changes the resistance of the device. Simultaneously, in order to detect the change in resistance, the thermistor is pulsed by an electrical signal. Thus, the current induced to flow through the bolometer is the output of interest.

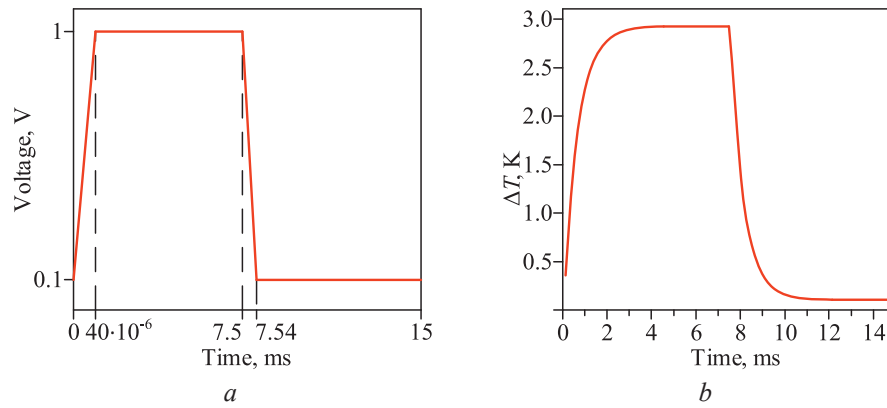


Fig. 7. Applied voltage profile for transient analysis (a) and dependence of temperature changes on time (b)

When the radiation abates and the bias voltage is removed, the sensor cools down with a characteristic time constant. The strategy employed here is pulsed biasing, in which the detector bias is applied only for a short period of time. Pulse biasing, as opposed to a continuous bias strategy, prevents possible damage to the pixels due to excessive joule heating as the self-heating is expected to be minimal. The applied voltage and heat flux input profile is shown in Fig. 8, a.

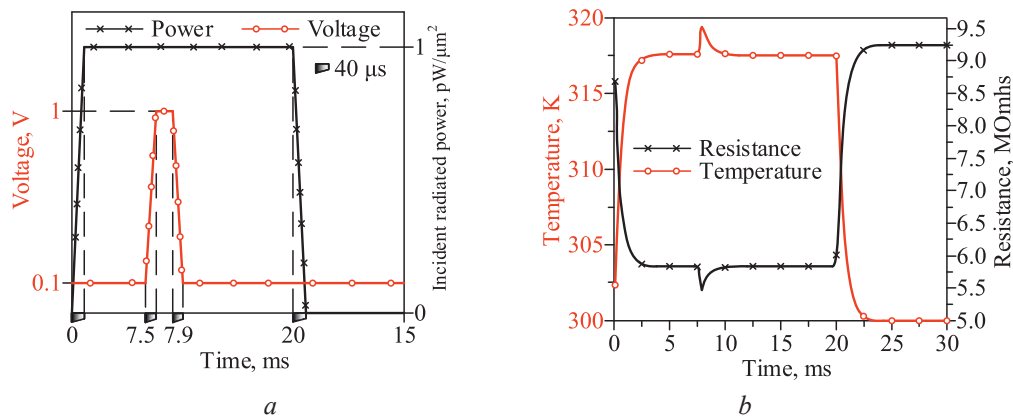


Fig. 8. Applied voltage and heat flux profiles for transient analysis (a) and dependence of temperature and microbolometer resistance on time (b)

The plot Fig. 8, b shows that the microbolometer first responds to the heat flux boundary condition, mimicking the power input from the absorption of radiation impinging the sensor. The temperature of the bolometer increases to a steady value of 317.5 K. The short voltage pulse is then applied after the sensor, temperature stabilizes from the heat input, and the temperature increases momentarily due to Joule heating, achieving a maximum temperature of 319.5 K. Once the voltage is turned off and the contribution from Joule heating is removed, the temperature drops to the local maximum corresponding to only the heat flux input. When heat flux is turned off, the temperature drops to 300 K, as defined by the heat sink. The plot Fig. 8, b shows that as the temperature of the sensor increases, the resistance decreases. This is consistent with the electrical conductivity values supplied for the α -Si thermistor layer. The impact on the resistance due to Joule heating is evident at 7.5 ms when the voltage pulse is applied. The difference in resistance between the quasi-steady-state value due to the temperature increase from the incidence radiation and the additional resistance due to self-heating represents an error in the measurements and should be minimized.

Conclusions

Mechanical robustness of focal plane area is very important to maintain infrared absorption performance as the microbolometer pixel size is decreased. In this paper, new structures have been designed and characterized to determine the influence of geometry on the characteristic parameters of a bolometer. The width and length of the support arm greatly affects the thermal conductivity of the device. The deformation of the device is controlled by a number of NiCr absorption layers and the thickness of the thermoelectric material. In conclusion, mechanical robustness of focal plane array related

to the infrared absorbance can be implemented by optimization of residual stress and alignment accuracy of each layer constituting the focal plane array. By the optimization of the fabrication process, we obtained a focal plane array with good mechanical robustness. This shows that the proposed pixel design is very useful for most applications.

References

1. Wood R. A., Han C. J., Kruse P. W. (1992) Integrated Uncooled Infrared Detector Imaging Arrays. *Solid-State Sensor and Actuator Workshop, 5th Technical Digest. IEEE*. 132–135.
2. Takamuro Daisuke, Tomohiro Maegawa, Takaki Sugino (2011) Development of New SOI Diode Structure for Beyond 17 μm Pixel Pitch SOI Diode Uncooled IRFPAs. *Proceedings of SPIE – the International Society for Optical Engineering*. 8012, 80121E.
3. Li C., Han C. J., Skidmore G. D., Hess. C. (2010) DRS Uncooled VO_x Infrared Detector Development and Production Status. *Proc SPIE*. 7660, 76600V.
4. Biao Li (2004) Design and Simulation of an Uncooled Double-Cantilever Microbolometer with the Potential for $\sim \text{mK}$ NETD. *Sensor and Actuators A: Physical*. 112 (2), 351–359.
5. Sedky S., Fiorini P., Caymax M., Agnes V., Baert C. (1998) IR Bolometers Made of Polycrystalline Silicon Germanium. *Sensors and Actuators A*. 66 (1–3), 193–199.
6. Heredia-J. A., Torres-J. A., De la Hidalgo-W. F. J., Jaramillo-N. A. (2002) A Boron Doped Amorphous Silicon Thin-Film Bolometer for Long Wavelength Detection. *Mat. Res. Soc. Symp. Proc.* (744), M5.26.1–M5.26.6.
7. Kosarev A., Moreno M., Torres A., Zuñiga C. (2008) IR Sensors Based on Silicon–Germanium–Boron Alloys Deposited by Plasma: Fabrication and Characterization. *J. of Non-Crystalline Solids*. 354 (19–25), 2561–2564.
8. Tisse C.-L., Tissot J.-L., Crastes A. (2012) An Information-Theoretic Perspective on the Challenges and Advances in the Race Toward 12 μm Pixel Pitch Megapixel Uncooled Infrared Imaging. *Proceedings of the SPIE*. 8353.
9. Hee Yeom Kim, Kyoung Min Kim, Byeong Il Kim et al. (2011) Mechanical Robustness of FPA in a-Si Microbolometer with Fine Pitch. *Sensors & Transducers Journal* (11), 56–63.
10. Abbasi S., Shafique A., Ceylan O., Kaynak C. B., Kaynak M., Gurbuz Y. (2018) A Test Platform for the Noise Characterization of SiGe Microbolometer ROICs. *IEEE Sensors Journal* (18), 6217.
11. Mottin E., Bain A., Martin J. L., Ouvrier-Buffet J. L., Bisotto S., Yon J. J., Tissot J. L. (2003) Uncooled Amorphous Silicon Technology Enhancement for 25 μm Pixel Pitch Achievement. *Proceedings of the SPIE*. 4820, 200–207.
12. Murphy D., Ray M., Wyles J., Asbrock J., Hewitt C., Wyles R., Gordon E., Sessler T., Kennedy A., Baur S., Van Lue D. (2004) Performance Improvements for VO_x Microbolometer FPAs. *Proceedings of the SPIE*. 5406, 531–540.

Authors' contribution

Tran Van Trieu analyzed the existing design solutions and conducted a simulation of the operational characteristics of the microbolometer.

Stempitsky V. R. established the task for the research, prepared the manuscript of the article.

Lovshenko I. Yu. interpreted the simulation results, prepared the manuscript of the article.

Korsak K. V. analyzed the design solutions used for the MEMS microbolometers.

Dao Dinh Ha performed a simulation of the operational characteristics of the microbolometer.

Information about the authors

Tran Van Trieu, Postgraduate of Micro- and Nanoelectronics Department of the Belarusian State University of Informatics and Radioelectronics; **Stempitsky V. R.**, Cand. of Sci., Associate Professor, Vice-Rector for Academic Affairs, Adviser of Laboratory “CAD in Micro- and Nanoelectronics” at the Research Department of the Belarusian State University of Informatics and Radioelectronics; **Lovshenko I. Yu.**, Head of the Research Laboratory “CAD in Micro- and Nanoelectronics” at the Research Department of the Belarusian State University of Informatics and Radioelectronics; **Korsak K. V.**, Master’s Student at the Micro- and Nanoelectronics Department of the Belarusian State University of Informatics and Radioelectronics; **Dao Dinh Ha**, Cand. of Sci. of the Le Quy Don University of Science and Technology.

Address for correspondence

220013, Republic of Belarus,
Minsk, P. Brovki St., 6
Belarusian State University
of Informatics and Radioelectronics
Tel.: +375 17 293-88-90
E-mail: lovshenko@bsuir.by
Lovshenko Ivan Yur’evich